

AD-A073 009

CORNELL UNIV ITHACA N Y SCHOOL OF ELECTRICAL ENGINEERING F/G 20/12
TRANSIENT PHENOMENA IN ELECTRON TRANSPORT IN SEMICONDUCTORS. (U)
JAN 79

AFOSR-74-2717

UNCLASSIFIED

AFOSR-TR-79-0928

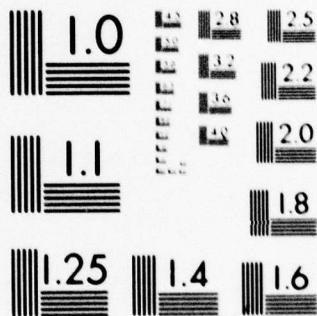
NL

1 OF 1

AD
A07 009



END
DATE
FILMED
9-79
DDC



MICROCOPY RESOLUTION TEST CHART
NATIONAL BUREAU OF STANDARDS-1963-A

DA 073009

18 AFOSR TR-79-0928

19

12

SC

LEVEL II

Approved for public release;
distribution unlimited.

6 TRANSIENT PHENOMENA IN
ELECTRON TRANSPORT IN SEMICONDUCTORS

15 AFOSR-74-2717

FINAL SCIENTIFIC REPORT

31 JAN 1979

12 227

11

DDC
REF ID: A6231979
RECEIVED

9 Final rept. for period ending 31 Jan 79.

Cornell Univ., Ithaca, N.Y.
School of Electrical Engineering

Approved for public release;
distribution unlimited.

79 08 22 045

098 850

mt

DDC FILE COPY

Final Scientific Report
Grant AFOSR-74-2717
period ending 31 January 1979

I. ABSTRACT

Theoretical efforts at understanding the band structure of, and hence electron transport in, alloy semiconductor materials are described. In particular, calculations of band structure and transient and equilibrated velocity-field relationships are being performed for $\text{Ga}_{(x)}\text{In}_{(1-x)}\text{As}$ and $\text{Ga}_{(k)}\text{In}_{(1-x)}\text{As}_y\text{P}_{(1-y)}$ materials which may be suitable for fast logic or microwave devices. Methods for describing pseudopotential variations and chemical disorder in alloys are discussed.

II. INTRODUCTION

Approximate calculations of velocity-field curves¹⁷ have indicated that the alloy semiconductors $\text{Ga}_{.47}\text{In}_{.53}\text{As}$ and $\text{Ga}_{.47}\text{In}_{.53}\text{As}_{.6}\text{P}_{.4}$, which can be epitaxially matched to GaAs or InP substrates, have a higher low-field mobility and peak velocity than GaAs. These properties may lead to improved microwave or fast logic devices, although experimental results on GaInAsP microwave FET's have been disappointing²⁵.

The work covered by this grant is an attempt to better describe the transport properties of these alloy materials.

To improve this description, it is first necessary to examine their band structures in greater detail than has been done before. Considerable difficulty arises in such an investigation, however, and some of the difficulties are described in this report.

III. Band Structures for III-V Semiconductors

A computer program was written and successfully applied to the calculation of band structures for III-V compounds using nonlocal pseudopotentials. This initial phase of the project was undertaken as a test of computer algorithms, with the intent of reproducing the results of Chelikowski and Cohen¹. The band structure calculation we performed generates two types of information:

1. Band energies as functions of wave vector. From this information, one can extract the following material properties needed for transport calculations:

- A. Fundamental gap, useful for characterization of heterojunctions and rough estimates of breakdown field.

- B. Band shape near conduction band minima, needed for equations of motion in transport simulations.

- C. Density of states, needed to calculate scattering rates.

- D. Sub-band gaps, needed for simulating

intervalley transfer.

2. Pseudo-wave functions. These functions are used in subsequent calculations to yield many necessary quantities, including:

- A. Intervalley scattering rates for transport simulations.
- B. Coupling strengths, which could be useful in the development of a complete theory of alloy scattering.
- C. Matrix elements for a wide variety of other transitions, such as photoabsorption and impact ionization.

We verified our computer program by calculating the band structure of GaP at symmetry points Γ , L and X, and comparing with published results:

Level	Energy (eV)	
	This work	Ref. 1
Γ_6^v	-13.00	-12.99
Γ_8^v	0	0
Γ_6^v	2.90	2.88
Γ_8^c	5.22	5.24
X_6^v	-9.47	-9.46
X_6^v	-7.07	-7.07
X_7^v	-2.73	-2.73
X_5^c	2.14	2.16
X_7^c	2.70	2.71

Accession For	
NTIS GAA&I	<input checked="" type="checkbox"/>
DDC TAB	<input type="checkbox"/>
Unannounced	<input type="checkbox"/>
Justification	
By _____	
Distribution/	
Availability Codes	
Dist	Avail and/or special
A	

L_6^V	-10.61	-10.60
L_6^V	-6.85	-6.84
$L_{4,5}^V$	-1.10	-1.10
L_6^C	2.79	2.79
$L_{4,5}^C$	5.72	5.74

IV. Band Structures for Alloy Semiconductors

Calculations of alloy band structures by others²⁻⁶ have involved several approximations. For example, all have used local pseudopotentials, which results in equal treatment of the wave function components of various angular momenta. Also the energy dependence of the pseudopotential operator has been ignored. These calculations appear to be inconsistent with experimental data, indicating that a nonlocal operator may be necessary for alloys⁴. These inconsistencies will be discussed later. Reinforcement for this statement is furnished by the report⁷ that nonlocal contributions are important in the calculation of intervalley phonon coupling constants, even for the compound semiconductors.

In an "empirical" band structure calculation, i.e., one in which the pseudopotential parameters are adjusted to give reasonable agreement between calculated and measured spectral properties, the nonlocal method requires more parameters than the local method. Fortunately, these

nonlocal parameters have already been determined¹ for a large number of III-V compounds in a manner that is apparently sufficiently accurate for the determination of input parameters for transport simulations.

We have developed techniques for interpolation of the local part of the pseudopotential across alloy composition ranges. The empirically determined form factors $V(k)$ for each compound at its equilibrium lattice constant are subjected to a nonlinear transformation² to remove the screening, then fitted to the three-parameter model function

$$V(k)=A(k-B)\exp(-C(k-B)).$$

This model function is then evaluated at wave numbers appropriate to the lattice constant of the alloy, and renormalized with respect to the atomic volume of the alloy. The form factors for the two or four compounds (for a ternary or quaternary alloy, respectively) are linearly interpolated according to the alloy composition ratio(s), and screening is reapplied.

Two techniques were developed for interpolating the nonlocal part of the pseudopotential in alloy systems. Unfortunately, neither has yet given results which can be accepted with confidence.

In the first technique, the cubes of the nonlocal radii (R^3) were linearly interpolated; the strength parameters α and β were then renormalized with respect to R^3 , and

subsequently interpolated. For a ternary alloy,

$$R_{\text{alloy}}^3 = xR_a^3 + (1-x)R_b^3$$

$$(\alpha)_{\text{alloy}} = x(\alpha)R_a/R_{\text{alloy}} + (1-x)(\alpha)R_b/R_{\text{alloy}},$$

where x is the composition ratio.

This method is inspired physically by the fact that in most of the matrix elements of the nonlocal operator, the nonlocal parameters enter as $(\alpha + f_\beta)R^3$, so the net nonlocal strength should be approximately preserved if α and β are scaled along with R^3 .

Calculations on $\text{Ga}_{.47}\text{In}_{.53}\text{As}$ using this scheme resulted in a bandgap $E_0 = 0.97$ eV (corrected for spin orbit splitting), higher than the measured value of 0.80 eV. Part of this difference may be attributable to neglect of alloy compositional disorder in the calculation, which uses the "virtual crystal" approximation (VCA). A disorder correction term can be added to the VCA energies, which results² in a decrease of the calculated gap to about 0.95 eV. We conclude that either our VCA calculations are in error, or the published results for the disorder effects are inaccurate, possibly due to the fact that they were found from a local pseudopotential.

In order to verify the correctness of our VCA calculations, a second nonlocal pseudopotential interpolation scheme, which involves calculating each matrix element separately for each compound then performing the linear interpolation on the matrix elements, was tried:

$$\langle k-G_i | H_{\text{alloy}}^{\text{nonlocal}} | k-G_j \rangle =$$

$$x\langle k-G_i | H_a^{n,l} | k-G_j \rangle + (1-x)\langle k-G_i | H_b^{n,l} | k-G_j \rangle$$

where $|k-G\rangle$ is a plane wave basis state.

This formula correctly scales the nonlocal terms only for the alloy atomic volume, not for the change in screening. However, screening may not be important for the nonlocal part of the potential¹.

Renormalization of R to account for the lattice constant change has been considered, but was not done because the available methods (such as a quadratic variation⁹ or the linear "touching spheres" criterion¹) would require previous knowledge of the band structure for each alloy composition. Since the results are relatively insensitive¹³ to the value of R as long as α and β are chosen appropriately, R was left unchanged from its value in the binary compound. The results for GaInAs using this second interpolation paradigm were nearly identical to the previous results.

On the basis of the above results, it was decided that new calculations of the disorder effect should be performed, using the nonlocal pseudopotential, in order to

1. satisfy the goal of calculating accurate sub-band gaps for alloys, and
2. determine whether the alloy pseudopotential is being properly formulated, thereby establishing a confidence level for the matrix elements that will be derived from the wave functions, even though there are presently no plans to correct the wave functions for disorder

effects. Until the energy band results (VCA+disorder) are made to agree with measurements, there is no guarantee that the VCA pseudowave functions are accurate.

There is considerable confusion in the literature regarding the disorder effect. Some authors^{5,10} appear to have obtained good agreement with experiment by ignoring disorder, while others^{11,12} have stressed the importance of disorder, particularly for anionic mixtures such as GaAsP. A local pseudopotential calculation¹⁵ of the disorder-induced bowing of the direct gap in GaAsP shows it to be nearly equal to the observed bowing, implying that the VCA bowing should be nearly zero. However, our local pseudopotential calculation of VCA bowing gives -0.46 eV. It is commonly agreed that disorder is relatively unimportant in AlGaAs⁴ and AlGaSb¹³, but there is some debate regarding GaInAsP. Some treatments¹² assume that disorder affects the entire Brillouin zone with the same strength while others¹¹ claim that some points are more strongly affected than others. Altarelli¹⁴ states that disorder is more important for the conduction band than for the valence band, while Baldereschi and Masonke¹⁵ find that the reverse is true. The latter work also conflicts with Stroud's claim¹¹ that disorder always reduces the gap relative to the VCA value. The evaluation of band structure calculation techniques for alloys is hindered by

the proliferation of incorrect pseudopotential parameters¹³ and by the spread in experimental data.

V. Density of States Calculations

To reduce computation time during transport simulations, a two-band secular equation model was applied to the "camel's back" conduction band structure¹⁶ at the X symmetry point, and expressions were derived for energy dispersion relations and density of states. The model is used by fitting to several points from the full pseudopotential calculation.

For GaInAsP compositions rich in As and In, the Δ minimum is expected to be at X and the dispersion relation is nearly parabolic. For compositions rich in Ga and P, the minimum shifts toward Γ and the band shape is approximately

$$E(k) = Ak_1^2 + Bk_t^2 - [(\Delta/2)^2 + \Delta_0 Ak_1^2]^{1/2}$$

where k_1 and k_t are the components of k (measured with respect to X) parallel and perpendicular, respectively, to the line. $A = \hbar^2/2m_1$, $B = \hbar^2/2m_t$.

The density of states is given by

$$g(E) = \frac{m_t}{\pi^2 \hbar^2 \sqrt{2A}} (\sqrt{x+y} - u_{-1}(x-y)\sqrt{x-y})$$

where $x = \Delta_0 - 2(E_0 - E)$,

$$y = \sqrt{\Delta_0^2 + \Delta^2 + 4\Delta_0(E - E_0)}$$

u_{-1} = unit step function.

The parameters Δ , Δ_0 , E_0 , A and B are obtained by fitting

to calculated band shapes.

V. CONCLUSIONS

A computer program was developed for the purpose of calculating band structures for III-V compounds using nonlocal pseudopotentials. Upon verification, these techniques were extended to band structure calculations of III-V alloys, but the results cannot yet be reconciled with experimental data. Additional calculations are now being performed for that purpose.

A large body of experimental measurements is available for comparison with calculated results, including energy gaps²¹, effective masses¹⁹, and high-field electron transport data²⁰.

A possible cause of disagreement between theory and experiment is the preferential clustering (also called segregation or short-range order) which has been observed in alloys. There have been theoretical attempts aimed at predicting the extent of this phenomenon²², and segregation has been observed, for example, in Bridgman-grown bulk GaInP²³. The influence of short range order on band structures has been studied²⁴ for binary systems, where the effect was described as "striking," and the extension to pseudo-binary systems like GaInAsP should be feasible. The effect of segregation as an additional scattering mechanism

(perhaps to be used in place of the usual "alloy scattering" term which was derived on the assumption of no segregation) has been introduced into electron transport simulations²⁵.

We consider the following topics to be worthy of further study:

1. Disorder contributions to the band structures of alloys. The validity (or invalidity) of the virtual crystal approximation should be definitively established.
2. Alloy scattering. Accurate methods should be established to replace the educated guesses¹⁷ which have been used to determine the strength of this process.
3. Interpolation methods for pseudopotential parameters should be studied more thoroughly. The various model potentials, such as square well, Gaussian well, and $1/r$, should be compared systematically.
4. Short range order in alloys should be investigated experimentally for various crystal growth conditions, and the results should be incorporated into band structure and transport calculations.

VI. REFERENCES

1. J. R. Chelikowski and M. L. Cohen, Phys. Rev. B 14, 556 (1976)
2. K.-R. Schulze, H. Neumann and K. Unger, Phys. Stat. Solidi (b) 75, 493 (1976)
3. F. Bassani and D. Brust, Phys. Rev. 131, 1524 (1963)
4. A. Baldereschi et al, J. Phys. C 10, 4709 (1977)
5. D. Jones and A. H. Lettington, Sol. State Comm. 7, 1319 (1969)
6. D. Richardson, J. Phys. C 4, L289 (1971)
7. D. C. Herbert, J. Phys. C 6, 2788 (1973)
8. A. Onton, Festkorperprobleme XIII, 59 (1973)
9. B. Welber et al, Phys. Rev. B 12, 5729 (1975)
10. R. Hill, J. Phys. C 7, 521 (1974)
11. D. Stroud, Phys. Rev. B 5, 3366 (1972)
12. O. Berolo et al, Phys. Rev B 8, 3794 (1973)
13. H. Mathieu et al, Phys. Rev B 12, 5346 (1975)
14. M. Altarelli, Solid State Comm. 15, 1607 (1974)
15. A. Baldereschi and K. Maschke, Solid State Comm. 16, 99 (1975)
16. P. Lawaetz, Solid State Comm. 16, 65 (1975)
17. M. Littlejohn et al, Sol. State Elec. 21, 107 (1973)
18. K. C. Pandey and J. C. Phillips, Phys. Rev. B 9, 1552 (1974)
19. J. B. Restorff et al, to be published
20. B. Houston et al, to be published in J. Solid State

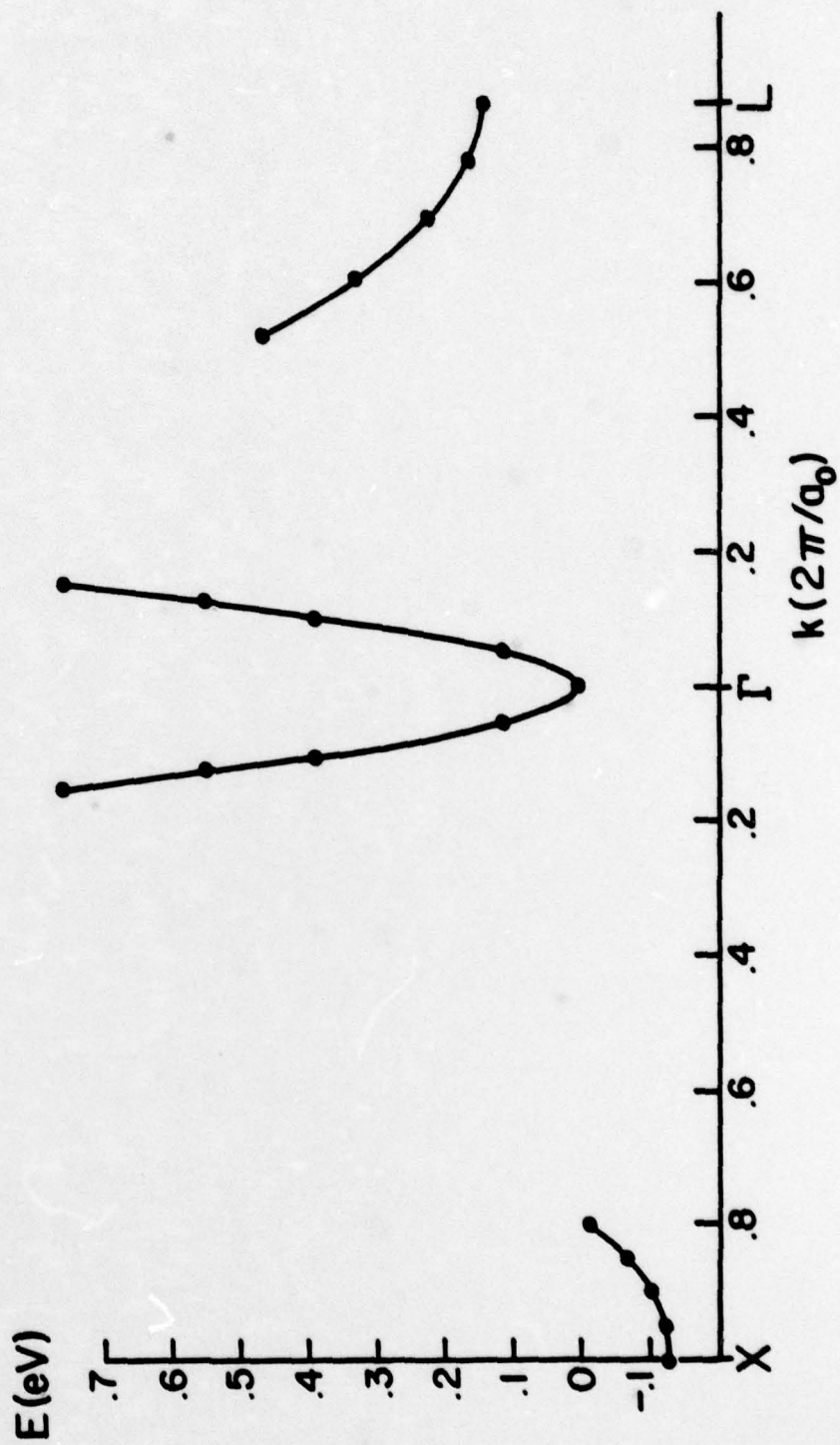
Electronics

21. K. Nakajima et al, Japan J. Applied Phys. 49, 5944 (1978)
22. A. A. Katsnelson et al, Phys. Stat. Solidi (b) 91, 11 (1979)
23. H-G. Brühl et al, Phys. Stat. Solidi (a) 39, 133 (1977)
24. L. M. Falicov, Phys. Rev. B. 12, 5664 (1975)
25. F. Oosaka et al, Japan J. Applied Phys. 15, 2371 (1976)
26. H. Morkoç et al, Elec. Letters 14, 443 (1978)

APPENDIX I

SAMPLE ALLOY SEMICONDUCTOR BANDSTRUCTURE CALCULATION

GaAs_{0.5}P_{0.5} VCA
Energy vs Wave Vector
Nonlocal Pseudopotential



APPENDIX II
PUBLICATION SUMMARIZING SOME OF THE EARLIER RESULTS
OF THIS WORK

Transient velocity characteristics of electrons in GaAs with Γ -L-X conduction band ordering^a

S. Kratzer and Jeffrey Frey

School of Electrical Engineering, Cornell University, Ithaca, New York 14853
(Received 10 February 1978; accepted for publication 1 March 1978)

The transient velocity characteristics of electrons in GaAs have been calculated for uniform electric fields at room temperature. Three-level band-structure data have been used with a Monte Carlo simulation program to predict electron drift velocity, temperature, and valley population fractions as functions of position and electric field. Results for two three-level band-structure models are compared with those for the previously accepted two-level model. Transient and steady-state properties are seen to be sensitive to some material parameters whose values are still in dispute.

PACS numbers: 72.80.Ey, 72.20.Ht

The performance of very small electron devices, such as microwave-field-effect transistors, may well be affected by the transient electron transport properties of the semiconductor materials of which they are made. This paper describes an investigation of some of the transient properties of electrons in GaAs, using recently published data¹ concerning the three-level band structure of this material and the processes that scatter electrons among the levels.

I. INTRODUCTION

The necessity for this work arises from new information on the band structure of GaAs. Previous calculations of the transient response of electrons in this material²⁻⁴ used a two-level band-structure model which, in the light of new experimental results, is now taken to be incorrect. This two-level model (hereafter called model T) placed the X minima of the conduction band at a lower energy than the L minima, and the L-X separation was assumed to be large enough so that scattering to the L valleys did not occur. In contrast, the new data, obtained by electroreflectance⁵ and other techniques,⁶ have been interpreted recently to show that the correct sequence, in order of increasing energies, is Γ -L-X; further, the intervalley separations are small, so that scattering among all valleys must be considered. Several authors^{1,6} have reported theoretical calculations which imply that the new band-structure model can be consistent with the observed steady-state transport properties of GaAs. We recall that, as early as 1970, Fawcett, Boardman, and Swain⁷ expressed consternation over the fact that some experimental results were inconsistent with model T.

It is possible to study the transient behavior of electrons in small devices by solving the differential equations describing conservation of energy and momentum.^{8,9} However solution of these equations becomes simple only when some extreme simplifications, such as the use of relaxation times derived from steady-state distribution functions are made. The accuracy of the results using this technique, therefore, is questionable. The preferred method is the more accurate but more costly one of Monte Carlo simulation, described elsewhere.⁷ The transient properties are calculated

here, using this method, for electrons in GaAs under the influence of a uniform electric field. The scattering processes included in the transport model are acoustic phonon through deformation potential, polar optic phonon, intervalley, ionized impurity, and (for the L valleys only) nonpolar optic phonon.

II. MATERIAL PARAMETERS

Values of the electron-lattice interaction parameters of GaAs for this calculation were obtained by critically examining all available data, which for some parameters cover a wide range. In Table I, column T represents the two-valley model used for previous transient calculations.²⁻⁴ Column B shows values obtained

TABLE I. Parameters for two-level (T) and three-level (B, C) models for the band structure of GaAs.

Parameter	Units	T ^a	B ^b	C	Alternatives
$m_{\Gamma, C}^*$	m_0		0.222	0.128	0.35, ^c 0.17 ^d
$m_{L, C}^*$	m_0	0.35	0.58	0.58	0.35, ^c 0.33 ^d
$m_{\Gamma, D}^*$	m_0		0.222	0.244	0.35, ^c 0.26 ^d
$m_{L, D}^*$	m_0	0.35	0.58	0.58	0.35, ^c 0.43 ^d
$E_{\Gamma L}$	eV		0.33	0.30	0.38, ^c 0.285, ^e 0.29 ^f
$E_{\Gamma X}$	eV	0.36	0.522	0.48	0.40, ^c 0.33, ^g 0.485, ^f 0.36 ^h
$E_1(\Gamma)$	eV	7.0	7.0	7.0	
$E_1(L)$	eV		9.2	2.24	7.0 ^c
$E_1(X)$	eV	7.0	9.27	3.0	7.0 ^c
$\alpha(\Gamma)$	eV ⁻¹	0.576	0.610	0.610	
$\alpha(L)$	eV ⁻¹		0.461	0.461	
$\alpha(X)$	eV ⁻¹	0	0.204	0.204	
$D_{\Gamma L}$	10 ⁸ eV/cm		10	10	2.8 ^c
$D_{\Gamma X}$	10 ⁸ eV/cm	10	10	10	11, ^c 5 ^g
D_{LL}	10 ⁸ eV/cm		10	10	1.8 ^c
D_{XX}	10 ⁸ eV/cm	10	7	7	10, ^c 1.3 ^g
D_{LX}	10 ⁸ eV/cm		5	5	5.5 ^c

^aReference 7.

^bReference 1.

^cReference 6.

^dI. Topol, H. Neuman, and E. Hess, Phys. Status Solidi B 55, K47 (1973).

^eReference 5.

^fT. Sugeta, A. Majerfeld, A.K. Saxena, and P.N. Robson (unpublished).

^gL.W. James and J.L. Moll, Phys. Rev. 183, 741 (1969).

^hA.R. Hutson, A. Jayaraman, and A.S. Coriell, Phys. Rev. 155, 786 (1969).

^aWork supported by the U.S. Air Force Office of Scientific Research.

for a three-level model by Littlejohn *et al.*¹ in a procedure aimed at achieving a "best fit" between Monte Carlo simulations and steady-state drift velocity measurements. This model (B) was used as a starting point in our investigation of transport properties. We describe below the reasons for considering changes to some of the parameter values used in model B.

The effective masses for the satellite valleys in model B are isotropic; that is, the conductivity mass m_c^* and density-of-states mass m_D^* are taken as equal. However, electroreflectance measurements⁵ and pseudopotential calculations¹⁰ indicate that the *L* valleys are highly anisotropic. Therefore, in model C we have obtained values for m_L^* by correcting¹¹ the data of Ref. 5 for inversion asymmetry and coupling to higher conduction bands.

The subband gaps used in model B were taken from the most recent measurements (E_{TL} by high-pressure transport,¹² E_{LX} by electroreflectances⁵). An additional measurement, of E_{TX} by optical absorption,¹³ was not used in the formulation of model B. However, this neglected last measurement yields data subject to a higher degree of experimental control than that obtained by high-pressure transport. Further, the analysis of the electroreflectance structure leads to an uncertainty of 30 meV for E_{TX} .¹¹ Therefore, we have used what we believe are correctly weighted averages of all available data for the subband gaps in model C.

The acoustic deformation potentials of model B for the satellite valleys were obtained from measurements on indirect-gap materials. Such measurements can yield a wide range of values; for example, those for the *X* valleys of GaP range¹⁴⁻¹⁶ from 3.7 to 55 eV. Some authors^{17,18} have attempted to calculate the acoustic deformation potential from derivatives with respect to pressure of direct energy gaps, taking the deformation potential for the valence band as zero. However, Rode¹⁹ has noted that this procedure may be very inaccurate and can be justified only because this scattering mechanism is relatively unimportant in GaAs at room temperature. In the interest of rigor, therefore, the values of acoustic deformation potential for the *L* and *X* valleys in column C were obtained from the dielectric bond calculations of Camphausen *et al.*,²⁰ which include the strain dependence of the valence band edge.

It should be noted that the strained-crystal pseudopotential method of Tsay and Bendow²¹ could be useful for calculating acoustic deformation potentials of GaAs. However, these authors have not reported some of the data necessary for the calculation, viz, deformation potentials for the indirect gaps and the ionization potential. Yee and Myers²² also used a nonperturbative pseudopotential method to calculate the acoustic deformation potential for the Γ valley. The computations are relatively simple and could easily be extended to the satellite valleys. However, the additive arbitrary constant which arises in their band-structure calculation has not been shown to be volume independent. Therefore, as Harrison²³ points out, such calculations could be used to find deformation potentials of energy gaps, but not the deformation potential of the conduction band.

The nonparabolicity values for the *L* and *X* valleys of model B were taken to be isotropic and were calculated from pseudopotential band-structure predictions.¹⁰ Jacoboni *et al.*,² in their Monte Carlo simulation of high-field transport in the Δ valleys of Si, also used an isotropic nonparabolicity constant, but they obtained the value empirically rather than from a band-structure calculation. However, even if the effective masses for these valleys were isotropic at the symmetry points, the nonparabolicity constants would not be so. The band-structure curves, by convention, cover only a small part of the Brillouin zone. For the *L* valleys, only longitudinal variations are shown (Γ to *L*, but not *L* to *K* or *L* to *W*). The nonparabolicity value obtained from these data, therefore, is appropriate only for the longitudinal component of *k*. Paige,²⁵ in his analysis of the *L* valleys of Ge, assumed that nonparabolicity is significant only for the transverse component of *k*. James²⁶ suggests using a high-order polynomial in k_x , k_y , and k_z (rather than $|k|$) to account for the anisotropy of the nonparabolicity. This topic needs further investigation, but in the absence of complete calculations we have retained the values of model B.

Finally, we note that Adams *et al.*⁶ presented a complete model for GaAs material parameters. We did not use this model because it includes a value for m_L^* ($0.35m_0$), which apparently cannot be justified by any published experiment or calculation. In the trial-and-error fitting process used by these authors, an error in one parameter can lead to compensating errors in several others, so that nonphysical parameter values may result even while the end results of the calculations may agree with some experimental data.

In the results presented below, models T and B are compared in order to determine whether previous GaAs device analyses^{8,27} would be significantly altered by the use of a three-level material model. Models B and C are compared in order to demonstrate that the individ-

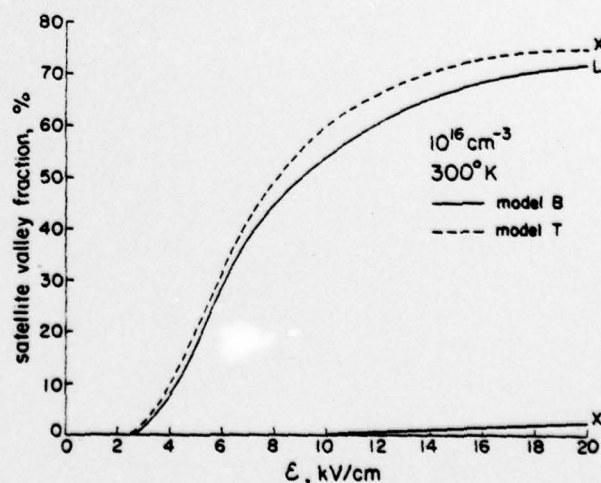


FIG. 1. Fraction of total electron density in each set of satellite valleys, as functions of electric field, for models T and B. $N = 10^{16}$, $T = 300$ K. For model C, *X* valley fraction is same as for model B; *L* valley fraction is nearly equal to *X* valley fraction of model T.

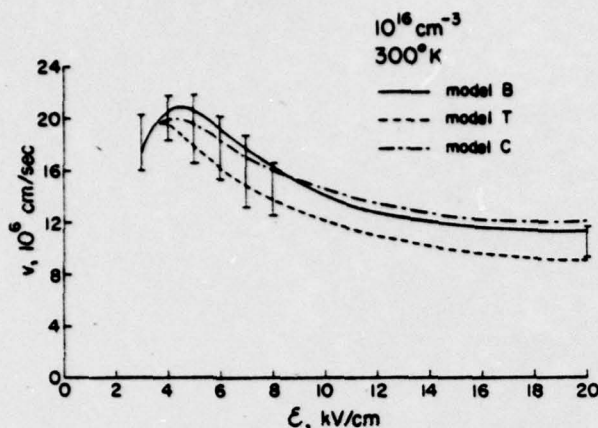


FIG. 2. Equilibrium drift velocity versus electric field for models T, B, and C; $N = 10^{16}$.

ual parameter changes described above have a substantial effect on the predicted transport properties. However, model C shares at least some of the failings of model B since the intervalley coupling constants and m_x^* values of model B, which were chosen to give reasonable steady-state properties in conjunction with the other parameters of this model, have been transferred to model C without alteration.

III. STEADY-STATE RESULTS

To obtain some information on the differences among models T, B, and C, we have calculated the steady-state transport properties using each model. Figure 1 shows that for model B the X valley population is quite small for fields up to 20 kV/cm. However, this does not mean that a two-valley (Γ - L) model would be adequate for low-field Monte Carlo simulations, because Γ - X - L transfers appear to be important in models B and C. Figure 2 shows that model C has a lower peak velocity and higher saturation velocity than model B, but both models yield results that fall within the range of experimental data, indicated by the bars in Fig. 2, up to about 10 kV/cm. At higher fields, model C gives a velocity that diverges from the results of model B and

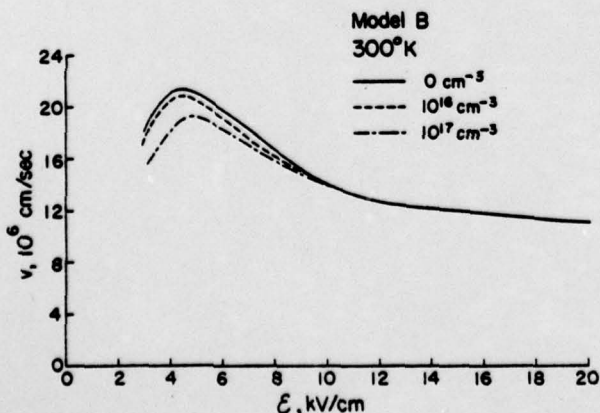


FIG. 3. Equilibrium velocity versus electric field for model B; $T = 300$ K, $N = 0, 10^{16}$, and 10^{17} .

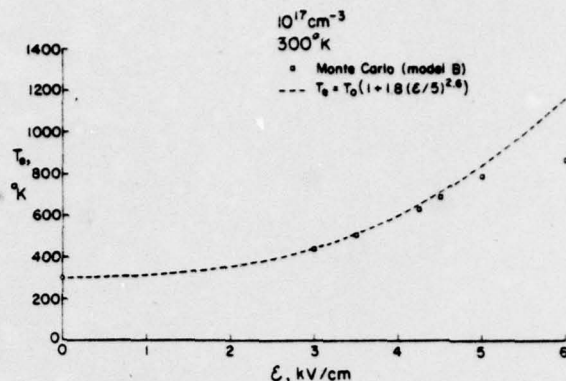


FIG. 4. Electron temperature versus electric field for model B; $N = 10^{17}$. Dashed line represents an empirical formula to be used for FET noise analysis.

from experiment, primarily because of the differences in m_x^* between the two models. The effect of doping on the steady-state properties of model B is shown in Fig. 3.

Electron temperature as a function of electric field is shown in Fig. 4, for model B. The three-level model (B) yields temperatures somewhat lower than does the two-level model (T), following the law $T_e = 300[1 + 1.8(E/5)^2.6]$ for $E < 4.5$ kV/cm. Therefore, GaAs transistors should have lower intrinsic noise figures than were previously predicted on the basis of the two-level model.²⁷ In fact, the latest GaAs FET noise results²⁸ do show this property. In addition, recent experimental results for GaAs layers²⁹ have shown a T_e -vs-electric-field relationship in agreement with that calculated here.

IV. TRANSIENT TRANSPORT BEHAVIOR

Figure 5 illustrates the velocity overshoot phenomenon for models T and B in terms of velocity versus distance for electrons which are initially in thermal equilibrium at 300 K. The field strengths of 10, 25, and 75 kV/cm have been taken as covering a range of values which may occur in field-effect transistors with gate lengths of 1 μ m or less.

Figure 6 shows the populations of the satellite valleys as functions of distance, for models T and B. At the

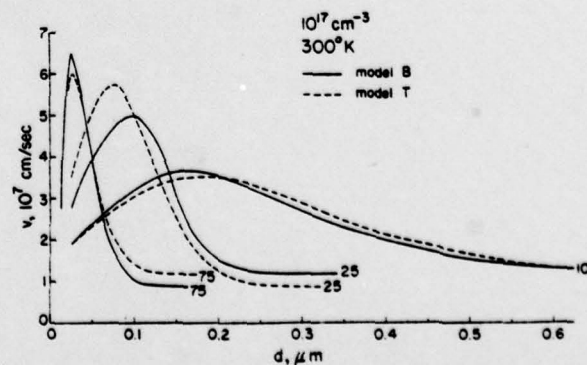


FIG. 5. Instantaneous velocity versus distance for models T and B; $N = 10^{17}$, $E = 10, 25$, and 75 kV/cm.

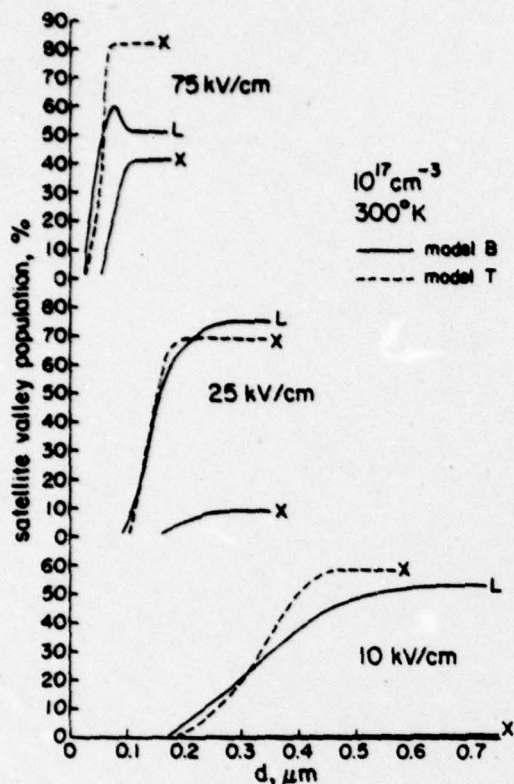


FIG. 6. Satellite valley fractions versus distance, for models T and B; $N = 10^{17}$, $E = 10, 25$, and 75 kV/cm.

higher field strengths, model B is seen to exhibit rapid transfer to the L valleys, via $\Gamma-L$ and $\Gamma-X-L$ transitions. After the L valley population has become significant, $L-X$ transfer causes the X valleys to become populated.

The effects of doping on the transient properties of model B are shown in Fig. 7. As previous authors have found for model T, impurity scattering has very little

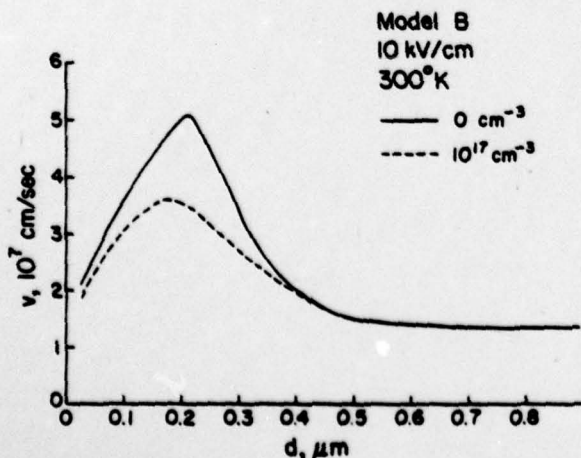


FIG. 7. Instantaneous velocity versus distance for model B; $E = 10$ kV/cm, $N = 0$ and 10^{17} .

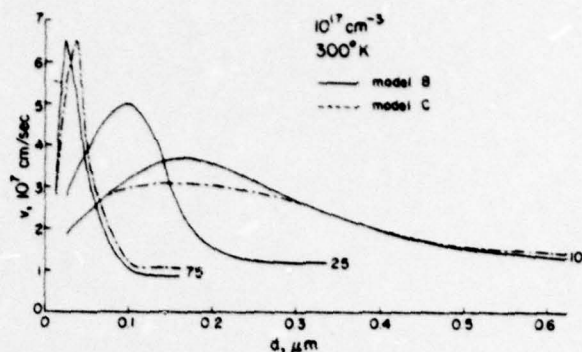


FIG. 8. Instantaneous velocity versus distance for models B and C; $N = 10^{17}$, $E = 10, 25$, and 75 kV/cm. At 25 kV/cm, the two curves are identical to within computational accuracy.

effect at high field strengths and causes a reduction in peak velocity at lower field strengths.

Figure 8 shows a comparison of transient responses for models B and C. At 10 kV/cm, the peak velocity of model B is 20% higher than that of model C, but at higher fields, the peak velocities are nearly equal.

V. CONCLUSIONS

The transient response of electrons in GaAs has been calculated using a now-discredited two-level band-structure model and two three-level models. A review of available data on material parameters has revealed some apparent inadequacies in individual parameters of one of the three-level models, which had been optimized as a set of parameters to yield steady-state properties which agree with experiment. Steady-state transport simulations suggest that the other three-level model, which was arrived at by consideration of the model parameters individually rather than as a complete set, is also not fully satisfactory. Nevertheless, the transient results presented herein should be useful in the further analysis of such GaAs devices as microwave-field-effect transistors.

The predicted transient properties are found to be quite sensitive to changes in the material parameters, even if we restrict our attention to those models that give good agreement with measured steady-state drift velocities. While this fact complicates the analysis of tiny electron devices when several material models are being considered, it also provides an opportunity to select from among these models when experimental transient results, as can be obtained by a microwave time-of-flight experiment,³⁰ become available.

ACKNOWLEDGMENTS

The authors wish to acknowledge helpful discussions with Professor C.A. Lee and Dr. T.J. Maloney. One of us (S.K.) is also grateful to the National Science Foundation for a Graduate Fellowship.

¹M. A. Littlejohn, J.R. Hauser, and T.H. Glisson, *J. Appl. Phys.* **48**, 4587 (1977).

- ¹J. Ruch, IEEE Trans. Electron Devices ED-19, 652 (1972).
- ²G. Hill, P. Robson, A. Majerfeld, and W. Fawcett, Electron. Lett. 13, 236 (1977).
- ³T. Maloney and J. Frey, J. Appl. Phys. 48, 781 (1977).
- ⁴D. E. Aspnes, Phys. Rev. B 14, 5331 (1976).
- ⁵A. R. Adams, P. J. Vinson, C. Pickering, G. D. Pitt, and W. Fawcett, Electron. Lett. 13, 46 (1977).
- ⁶W. Fawcett, A. D. Boardman, and S. Swain, J. Phys. Chem. Solids 31, 1963 (1970).
- ⁷M. Shur, Electron. Lett. 12, 615 (1976).
- ⁸R. Huang and P. Laidbrooke, J. Appl. Phys. 48, 4791 (1977).
- ⁹M. Cohen and T. Bergstresser, Phys. Rev. 141, 789 (1966).
- ¹⁰D. E. Aspnes (private communication).
- ¹¹D. E. Aspnes and M. Cardona (unpublished).
- ¹²A. Onton, R. Chloutka, and Y. Yacoby, *Proceedings of the Eleventh International Conference on the Physics of Semiconductors*, Warsaw, 1973 (unpublished).
- ¹³I. Balslev, *Proceedings of the International Conference on the Physics of Semiconductors*, Kyoto, 1966 (unpublished).
- ¹⁴A. S. Epstein, J. Phys. Chem. Solids 27, 1611 (1966).
- ¹⁵E. Haga and H. Kimura, J. Phys. Soc. Jpn. 19, 658 (1964).
- ¹⁶H. Ehrenreich, J. Phys. Chem. Solids 2, 131 (1957).
- ¹⁷D. L. Rode, *Semiconductors and Semimetals*, edited by R. Willardson and A. Beer (Academic, New York, 1975), Vol. 10, p. 87.
- ¹⁸D. L. Rode, Phys. Rev. B 2, 1012 (1970).
- ¹⁹D. Camphausen, G. Neville Connell, and W. Paul, Phys. Rev. Lett. 26, 184 (1971).
- ²⁰Y-F Tsay and B. Bendow, Phys. Rev. B 16, 2663 (1977).
- ²¹J. H. Yeo and G. Myers, Phys. Status Solidi B 77, K81 (1976).
- ²²W. A. Harrison, *Solid State Theory* (McGraw-Hill, New York, 1970), p. 391.
- ²³C. Jacoboni, R. Minder, and G. Majni, J. Phys. Chem. Solids 36, 1129 (1975).
- ²⁴E. S. B. Paige, Prog. Semicond. 8, 103 (1964).
- ²⁵L. W. James, J. Appl. Phys. 44, 2746 (1973).
- ²⁶J. Frey, IEEE Trans. Electron Devices ED-23, 1293 (1976).
- ²⁷W. W. Hooper, J. R. Anderson, H. F. Cooke, and M. Omori, IEEE International Electronic Devices Meeting, Washington, D. C., 1977 (unpublished).
- ²⁸J. Graffeuil (private communication).
- ²⁹T. J. Maloney, Ph.D. thesis (Cornell University, 1976) (unpublished).